Supporting Information

Douglas et al. 10.1073/pnas.1419133112

SI Text

Application of Multiple Homolog Mean Isotope Values

In most lake sediment samples, there are multiple plant wax homologs, i.e., plant waxes with different numbers of carbon atoms. Some studies have suggested that different plant taxa produce these plant waxes in different abundances (1, 2), but systematic taxonomic patterns are not well defined (3), and there is no consensus as to which homolog is the best indicator of hydroclimate change (δD_{wax}) or vegetation change ($\delta^{13}C_{wax}$).

In sediments from both Lake Chichancanab and Lake Salpeten, we observe substantial interhomolog variability in both δD and $\delta^{13}C$. In both cases, the C_{28} homolog is the most D-enriched, C_{26} is most D-depleted, and C_{30} typically has intermediate values (Tables S2 and S3). At both lakes, the C_{26} homolog is also typically the most ^{13}C enriched, whereas differences between the C_{30} and C_{28} homologs in terms of $\delta^{13}C$ values are less consistent between the two lakes (Tables S2 and S3). Interhomolog isotopic variability is evident in *n*-alkanoic acids from some plant extracts, but there are no clear patterns between plant taxa (4, 5). We suggest that the observed differences likely arise because of differences in the plant sources of these molecules. For instance, the high $\delta^{13}C$ values of the C_{26} *n*-alkanoic acid homolog suggest it is likely to have a relatively large source from C_4 grasses, whereas the C_{28} and C_{30} homologs likely have a larger source from C_3 flora.

In this study, we focused on the mean δD and $\delta^{13}C$ values of the C_{26}, C_{28}, and C_{30} homologs for two reasons. First, because of sample size limitations, our plant wax radiocarbon analyses were conducted on combined samples of the C_{26}, C_{28}, C_{30}, and C_{32} homologs. There may be small differences in the ages of these individual homologs, and therefore it is appropriate to apply a mean stable isotope value when using these ages to understand the chronology of plant wax stable isotope records. The C_{32} homolog was not sufficiently abundant for accurate stable isotope measurement in many samples and is not included in mean δD_{wax} and $\delta^{13}C_{wax}$ values. This homolog, however, represents a very small fraction of the compound-specific radiocarbon samples (typically less than 5%) and probably does not influence the age−depth models significantly.

Second, different *n*-alkanoic acid homologs likely vary in their dominant plant sources, which potentially differ in their D/H response to hydroclimate change. Because there is no good rationale for selecting a single homolog as the best indicator of climate or vegetation change, the mean δD and $\delta^{13}C$ values of these homologs provide the most general indicator of past environmental change. Analyses of soils and lake surface sediments from southeastern Mexico and Guatemala indicate that mean δD_{wax} values are significantly correlated with climate variables, in many cases to a greater degree than δD values of individual homologs (6).

In this study, we did not analyze abundance-weighted mean isotope values, because there is substantial temporal variability in the relative abundance of the C_{26}, C_{28}, and C_{30} homologs in these two cores. Because these homologs display large differences in their δD values, an abundance-weighted mean δD_{wax} record could be biased by variability in homolog relative abundance. In contrast, the unweighted mean value is not affected by homolog relative abundance. For consistency, we also applied unweighted mean $\delta^{13}C_{wax}$ records. Whereas the isotopic values of individual homologs are offset from one another, they display similar temporal patterns that are consistent with the evidence for climatic and vegetation changes inferred from the mean δD_{wax} and $\delta^{13}C_{wax}$ values.

Accounting for Differences in δD_{wax} Between Plant Groups

In addition to hydrological variables, δD_{wax} values can be influenced by differences in hydrogen isotope fractionation between different plant groups, with lower δD_{wax} in grasses than in trees and shrubs from the same environment (5, 7), and it is possible that vegetation change can bias the δD_{wax} record of climatic change (6). A recent study (8) proposed a method for applying $\delta^{13}C_{wax}$ data to correct δD_{wax} records for vegetation change in tropical environments dominated by C_3 trees and shrubs and C_4 grasses. This method applies ε_a (the apparent hydrogen isotope fractionation between plant-source water and plant waxes) values measured in C_3 trees and shrubs and C_4 grasses, as well as end-member $\delta^{13}C_{wax}$ values for these two groups, to develop a vegetation-corrected δD_{wax} ($\delta D_{wax\text{-}corr}$) value, using the following equations:

$$f_{c4} = \frac{\delta^{13}C_{wax} - \delta^{13}C_{c3}}{\delta^{13}C_{c4} - \delta^{13}C_{c3}} \qquad \textbf{[S1]}$$

$$\varepsilon_a = f_{c4}(\varepsilon_{c4}) + (1 - f_{c4})(\varepsilon_{c3}) \qquad \textbf{[S2]}$$

$$\delta D_{wax\text{-}corr} = \left[\frac{\delta D_{wax} + 1{,}000}{\left(\frac{\varepsilon_a}{1{,}000}\right) + 1}\right] - 1{,}000 \qquad \textbf{[S3]}$$

where f_{c4} is the estimated proportion of plant waxes derived from C_4 plants, $\delta^{13}C_{c3}$ and $\delta^{13}C_{c4}$ are end-member $\delta^{13}C_{wax}$ values for C_3 trees and shrubs and C_4 grasses, respectively, and ε_{c3} and ε_{c4} are end-member apparent D/H fractionation factors for C_3 trees and shrubs and C_4 grasses, respectively.

We slightly modified the calculations of ref. 8 to reflect that we analyze *n*-alkanoic acids as opposed to *n*-alkanes. To account for this difference, we applied $\delta^{13}C_{c3}$ (−37.1 ± 0.3‰), $\delta^{13}C_{c4}$ (−21.3 ± 0.7‰), ε_{C3} (−94 ± 4 ‰), and ε_{C4} (−122 ± 4 ‰) values based on measurements of *n*-alkanoic acids in C_3 trees and C_4 grasses from East Asia (5), the only study that has compared *n*-alkanoic acid isotope values in C_3 and C_4 plants grown with water of known isotopic composition. We calculated these end-member values as the mean of the C_{26}, C_{28}, and C_{30} homologs in that study. The listed errors are 1σ SEM. We calculated a combined error for $\delta D_{wax\text{-}corr}$ values of ±7‰ using a Monte Carlo method in Matlab that incorporated errors for the end-member values listed above, as well as analytical error for δD_{wax} (5‰) and $\delta^{13}C_{wax}$ (0.5‰). The error for $\delta D_{wax\text{-}corr}$ is insensitive to δD_{wax} and $\delta^{13}C_{wax}$ values.

$\delta D_{wax\text{-}corr}$ values roughly approximate the δD composition of plant water, although further study is required to assess how closely they approximate this value. Regardless, $\delta D_{wax\text{-}corr}$ values provide an indication of δD_{wax} variability that accounts for the influence of vegetation change. This technique is only applicable in environments where C_3 trees and shrubs and C_4 grasses are the dominant plant groups, and C_3 grasses and CAM plants are not abundant, as is the case in many low-elevation tropical regions with subarid to humid climates, including the Maya lowlands (9).

Applying the vegetation correction described above to the Lake Chichancanab and Lake Salpeten sediment cores, although shifting the overall δD value, does not produce an appreciably different record of climate variability (Fig. S1). This is because of the relatively modest degree of $\delta^{13}C_{wax}$ variability in these cores (<4‰), which indicates shifts in the relative abundance of C_3

and C_4 plants on the order of 20–30%, combined with large δD_{wax} variability (40–50‰).

$\delta^{13}C_{wax}$ as a Recorder of Ancient Maya Land Use

The $\delta^{13}C$ of plant waxes is strongly determined by the carbon isotope composition of bulk plant tissue (1, 2, 5). In the Maya Lowlands, where the dominant natural vegetation is C_3 angiosperm forest, but where there are large amounts of C_4 grasses (9), especially under circumstances of human disturbance, the relative proportion of C_3 to C_4 plants is the dominant control on $\delta^{13}C_{wax}$ values in lake sediments (10). The $\delta^{13}C_{wax}$ has similarly been applied as a robust indicator of the relative abundance of C_3 and C_4 plants in other tropical locations (11, 12).

In many natural settings, the relative abundance of C_4 grasses is largely controlled by climate, because C_4 plants have a competitive advantage over trees and shrubs under hot, dry conditions. In fact, glacial-to-interglacial $\delta^{13}C_{wax}$ from a number of locations, including the Maya Lowlands, have shown a strong dependence on climate (10, 11). Under ancient Maya land use regimes, however, climatic controls on C_3/C_4 vegetation dynamics are likely to have been diminished. The ancient Maya cleared large areas of C_3 deciduous and evergreen tropical forest, which led to a large increase in the abundance of C_4 grasses and other disturbance taxa (13, 14). Most palynological studies in the Maya Lowlands have found that human land use, as opposed to climate change, was the dominant driver of vegetation cover change during the late Holocene (13, 15). Furthermore, the staple crop of the ancient Maya was maize, a C_4 grass, and ancient agricultural settings in the Maya lowlands exhibit strong $\delta^{13}C$ enrichment of soil organic carbon (16, 17). Therefore, the relative abundance of C_4 plants, inferred from $\delta^{13}C_{wax}$ measurements, is interpreted primarily as an indicator of ancient Maya land use.

The transport pathways for plant waxes from terrestrial ecosystems to lake sediment are not well constrained. Analyses of δD_{wax} and plant wax radiocarbon ages ($\Delta^{14}C_{wax}$) in Lake Chichancanab sediments and catchment soils (18), however, indicate that in karst regions of the Maya Lowlands, they are primarily transported from catchment soils. The relatively old ^{14}C ages of plant waxes in lake surface sediments from the Maya Lowlands specifically argue against significant atmospheric input from aerosols (18). This means that sedimentary plant waxes are largely derived from within the lake catchment, and that $\delta^{13}C_{wax}$ values provide a local, catchment-integrated record of vegetation change. This is an important consideration in the context of the Maya Lowlands, where human land use led to high spatial variability in vegetation patterns (19, 20).

The ancient Maya practiced a wide range of land use strategies, including swidden agriculture, terraced upland agriculture, wetland agriculture, agroforestry, and garden orchards (19–22). Abundances of C_4 plants in the Lake Chichancanab and Lake Salpeten sediment cores were likely controlled by the spatial coverage of upland agriculture within the lake catchments. These two catchments do not contain sizeable wetlands aside from the lakes themselves and are therefore unlikely to have captured large amounts of plant waxes originating from wetland agricultural sites. Changes in the amount of land used for upland staple crop agriculture, which typically involves the burning or clearing of forests and their replacement with largely C_4 crops (19, 20), would probably account for the strongest signal of relative abundance of C_4 plants. Other land uses that emphasize C_3 plants, such as agroforestry or orchards (23, 24), would be less likely to affect the $\delta^{13}C_{wax}$ signal with respect to natural vegetation.

Archaeological and sedimentological data both indicate a much larger human presence at Lake Salpeten than at Lake Chichancanab, in terms of both the number of ancient residential structures surveyed (25) and the evidence for major anthropogenic soil erosion in the Lake Salpeten sediments (26), which is not present in Lake Chichancanab sediments (27). The presence of *Zea* pollen in a low-resolution palynological record from Lake Chichancanab, however, indicates maize agriculture did occur in its catchment (15). The similar $\delta^{13}C_{wax}$ records between the two catchments suggest that human land use effects on the abundance of C_4 plants were similar between the two catchments, despite the evidence for larger populations surrounding Lake Salpeten. This pattern is consistent with extensive swidden agriculture conducted by low-density populations leading to enhanced C_4 plant growth in both catchments during the Preclassic Period.

The palynological record from Lake Salpeten (14) provides a valuable comparison with the $\delta^{13}C_{wax}$ record from this lake (Fig. S4), although the pollen record has relatively low temporal resolution. The pollen record from Lake Salpeten has been interpreted as indicating a large increase in disturbance taxa, including grasses and weeds associated with anthropogenic deforestation, beginning in the early Preclassic period and lasting through the Terminal Classic, with a return to dominance of tropical forest taxa during the Postclassic period (14, 26, 28). This interpretation is partially at odds with the $\delta^{13}C_{wax}$ record, which indicates a decrease in C_4 plants during the Early Classic period, much earlier than the decline in disturbance taxa pollen. When the disturbance taxa are disaggregated, however, it is apparent that *Poaceae* (grass) pollen, the family accounting for most C_4 plants in the region, began to decline in the Late Preclassic (Fig. S4*B*). Given the low resolution of the pollen data, this decrease in *Poaceae* is consistent with evidence for decreasing C_4 plants in the Classic Period from the $\delta^{13}C_{wax}$ record. In contrast, other disturbance taxa such as *Asteraceae* and *Ambrosia,* which are dominantly C_3 plants, increased in abundance through the Classic period (Fig. S4 *C* and *D*). One explanation for these patterns, consistent with both the $\delta^{13}C_{wax}$ record and population estimates, is that during the Classic period, the predominant land use in the Lake Salpeten catchment shifted from low-population-density swidden agriculture, which promoted grasses, to higher-population-density residential land use that promoted the growth of C_3 disturbance flora including *Asteraceae* and *Ambrosia*.

Zea (maize) pollen is also present in Salpeten sediments in horizons spanning the late Preclassic to early Classic, including the period of minimum $\delta^{13}C_{wax}$ values (Fig. S4*B*). There are two key points in interpreting the presence of *Zea* pollen. First, *Zea* pollen is not abundant in the sediment core, and although its presence indicates maize agriculture, it does not provide strong evidence for the abundance of maize in the catchment (29). Second, *Zea* pollen grains have a relatively short transport distance (~200 m) (30, 31) and therefore primarily represent maize production close to the lake. We suggest that the continued presence of maize pollen in the lake sediments during the Classic period, concurrent with evidence for an overall decrease in C_4 plants in the lake catchment, suggests that maize agriculture did continue in the Salpeten basin, but at lower levels than occurred during the Preclassic. Maize cultivation in the catchment may have shifted from the hillslopes to the lakeshore during the Classic, a shift that could have enhanced the preservation of maize pollen in the lake sediments even as overall catchment C_4 plant abundance declined. This scenario would be consistent with the adoption of water-conservative agriculture in the Classic period, as agriculture near the lakeshore would have been better able to access the perched aquifer that feeds the lake, than would crops grown on the catchment hillslopes.

Age–Depth Models for Plant Wax Stable Isotope Records

Sediments from both Lakes Chichancanab and Salpeten contain a large proportion of pre-aged plant waxes, as indicated by plant wax ^{14}C ($^{14}C_{wax}$) ages that are significantly older than the age of sediment deposition based on ^{14}C dating of terrigenous macrofossils (Fig. 3). This age offset poses a complication for reconstructing past changes in plant wax stable isotope values, because terrigenous macrofossil (TM) age–depth models do not correspond to the time that the plant waxes were synthesized and their stable isotope values were recorded.

We addressed this complication by applying plant wax (PW) age–depth models that rely on compound-specific radiocarbon ages, as discussed in the Introduction. There are only two brief intervals in the upper meter of the Lake Salpeten sediment core in which the 95% confidence intervals of the PW and TM age models overlap (Fig. 3). The $^{14}C_{wax}$ ages in the Lake Salpeten core change by only 20 y between 262 cm and 147 cm depth, suggesting that the age of deposited plant waxes is essentially invariant across this stratigraphic interval, which was a time of very rapid sediment deposition (Fig. 3). Applying the PW age model to $\delta D_{wax\text{-}corr}$ and $\delta^{13}C_{wax}$ data from this interval of the sediment core results in data with very high temporal resolution (Fig. S2*B*) whose interpretation is relatively uncertain in the context of this study. We do not include these data in our analysis of $\delta D_{wax\text{-}corr}$ and $\delta^{13}C_{wax}$ records of past environmental change, which is focused on centennial-scale variability.

To assess the ability of the Lake Salpeten PW and TM age–depth models to accurately reflect the chronology of plant wax stable isotope variability, we compared $\delta D_{wax\text{-}corr}$ records fit to both of these age models with $\delta^{18}O$ records from Lake Salpeten (28) and the nearby Yok I speleothem from Belize (32) (Fig. S2). The δD_{wax} record fit to the PW age model (Fig. S2*B*) is in broad agreement with centennial climate variability evident in the Yok I speleothem $\delta^{18}O$ record (Fig. S2*C*). In contrast, the δD_{wax} record fit to the TM age model (Fig. S2*A*) is temporally offset from the Yok I speleothem $\delta^{18}O$ record.

The δD_{wax} record fit to the PW age model also records long-term trends toward wetter conditions from 3,200 y B.P. to 2,200 y B.P. and toward drier conditions from 1,800 y B.P. to 1,000 y B.P. that are apparent in the Lake Salpeten $\delta^{18}O$ record (Fig. S2*D*). The $\delta D_{wax\text{-}corr}$ record fit to the TM age model, in contrast, records a trend toward wetter conditions from 2,000 y B.P. to 1,200 y B.P. that does not agree with the Lake Salpeten $\delta^{18}O$ record. Although the Lake Salpeten $\delta^{18}O$ record has been interpreted to have been partially controlled by changes in runoff caused by anthropogenic deforestation and afforestation, it is likely that long-term trends in this record are in large part a consequence of changes in the ratio of evaporation to precipitation (28). In particular, the trend toward elevated $\delta^{18}O$ values beginning at ∼200 C.E. precedes pollen evidence for afforestation by at least 500 y (28), suggesting that it primarily reflects climatic change.

Similar results are found for Lake Chichancanab, with the δD_{wax} record fit to the PW age model providing a better fit to regional proxy records for hydroclimate from the northern Maya Lowlands (18). We also conducted an inverse modeling exercise to determine which plant wax age distributions provided the best fit between δD_{wax} and the 7,500-y gastropod $\delta^{18}O$ record from Lake Chichancanab (27). The best correspondence between these two records is achieved with plant wax age distributions in which the majority (>80%) of plant waxes are cycled on millennial time scales and the age variance of this millennially cycled pool of plant waxes is relatively small (<200 y) (18). This age distribution is consistent with the PW age model providing an accurate record of past δD_{wax} variability on millennial and centennial time scales.

Because of the lack of high-resolution, long-term (i.e., >3,500 y) climate records from the southern Maya Lowlands, the inverse modeling approach applied at Lake Chichancanab is not feasible at Lake Salpeten. Nevertheless, the Lake Chichancanab and Lake Salpeten catchments are both characterized by karst hydrology, and plant wax transport pathways and age distributions for the two lakes are probably similar. Furthermore, the presence of high-amplitude δD_{wax} variability in records from both lakes (18) (Fig. S2*B*) provides a strong argument against significant mixing of plant waxes of different ages and further supports the application of PW age models.

1. Rommerskirchen F, Plader A, Eglinton G, Chikaraishi Y, Rullkotter J (2006) Chemotaxonomic significance of distribution and stable carbon isotopic composition of long-chain alkanes and alkan-1-ols in C-4 grass waxes. *Org Geochem* 37(10):1303–1332.
2. Vogts A, Moossen H, Rommerskirchen F, Rullkotter J (2009) Distribution patterns and stable carbon isotopic composition of alkanes and alkan-1-ols from plant waxes of African rain forest and savanna C-3 species. *Org Geochem* 40(10):1037–1054.
3. Bush RT, McInerney FA (2013) Leaf wax *n*-alkane distributions in and across modern plants: Implications for paleoecology and chemotaxonomy. *Geochim Cosmochim Acta* 117:161–179.
4. Chikaraishi Y, Naraoka H (2007) $\delta^{13}C$ and δD relationships among three n-alkyl compound classes (n-alkanoic acid, n-alkane and n-alkanol) of terrestrial higher plants. *Org Geochem* 38(2):198–215.
5. Chikaraishi Y, Naraoka H, Poulson SR (2004) Hydrogen and carbon isotopic fractionations of lipid biosynthesis among terrestrial (C3, C4 and CAM) and aquatic plants. *Phytochemistry* 65(10):1369–1381.
6. Douglas PMJ, Pagani M, Brenner M, Hodell DA, Curtis JH (2012) Aridity and vegetation composition are important determinants of leaf-wax δD values in southeastern Mexico and Central America. *Geochim Cosmochim Acta* 97:24–45.
7. Sachse D, et al. (2012) Molecular paleohydrology: Interpreting the hydrogen-isotopic composition of lipid biomarkers from photosynthesizing organisms. *Annu Rev Earth Planet Sci* 40:221–249.
8. Collins JA, et al. (2013) Estimating the hydrogen isotopic composition of past precipitation using leaf-waxes from western Africa. *Quat Sci Rev* 65:88–101.
9. Sage RF, Wedin DA, Li M (1999) The biogeography of C4 photosynthesis: Patterns and controlling factors. *C4 Plant Biology*, eds Sage RF, Monson RK (Academic, San Diego), pp 313–373.
10. Huang Y, et al. (2001) Climate change as the dominant control on glacial-interglacial variations in C3 and C4 plant abundance. *Science* 293(5535):1647–1651.
11. Hughen KA, Eglinton TI, Xu L, Makou M (2004) Abrupt tropical vegetation response to rapid climate changes. *Science* 304(5679):1955–1959.
12. Huang YS, Dupont L, Sarnthein M, Hayes JM, Eglinton G (2000) Mapping of C_4 plant input from North West Africa into North East Atlantic sediments. *Geochim Cosmochim Acta* 64(20):3505–3513.
13. Wahl D, Byrne R, Schreiner T, Hansen R (2006) Holocene vegetation change in the northern Peten and its implications for Maya prehistory. *Quat Res* 65(3):380–389.
14. Leyden BW (1987) Man and climate in the Maya Lowlands. *Quat Res* 28(3):407–417.
15. Leyden BW (2002) Pollen evidence for climatic variability and cultural disturbance in the Maya lowlands. *Ancient Mesoam* 13(1):85–101.
16. Beach T, et al. (2011) Carbon isotopic ratios of wetland and terrace soil sequences in the Maya Lowlands of Belize and Guatemala. *Catena* 85(2):109–118.
17. Webb EA, et al. (2007) Stable carbon isotope signature of ancient maize agriculture in the soils of Motul de San Jose, Guatemala. *Geoarchaeology* 22(3):291–312.
18. Douglas PMJ, et al. (2014) Pre-aged plant waxes in tropical lake sediments and their influence on the chronology of molecular paleoclimate proxy records. *Geochim Cosmochim Acta* 141:346–364.
19. Turner BL, II, Sabloff JA (2012) Classic Period collapse of the Central Maya Lowlands: Insights about human-environment relationships for sustainability. *Proc Natl Acad Sci USA* 109(35):13908–13914.
20. Dunning NP, Beach T (2011) Farms and forests: Spatial and temporal perspectives on ancient Maya landscapes. *Landscapes and Societies*, eds Martini IP, Chesworth W (Springer, Dordrecht, The Netherlands), pp 369–389.
21. Dunning NP, et al. (2002) Arising from the bajos: The evolution of a neotropical landscape and the rise of Maya civilization. *Ann Assoc Am Geogr* 92(2):267–283.
22. Turner BL, II (1974) Prehistoric intensive agriculture in the Mayan Lowlands. *Science* 185(4146):118–124.
23. Lentz DL, Hockaday B (2009) Tikal timbers and temples: Ancient Maya agroforestry and the end of time. *J Archaeol Sci* 36(7):1342–1353.
24. Ross NJ (2011) Modern tree species composition reflects ancient Maya "forest gardens" in northwest Belize. *Ecol Appl* 21(1):75–84.
25. Rice DS, Rice PM (1990) Population size and population change in the central Peten lakes region, Guatemala. *Precolumbian Population History in the Maya Lowlands*, eds Culbert TP, Rice DS (Univ New Mexico Press, Albuquerque), pp 123–148.
26. Anselmetti FS, Hodell DA, Ariztegui D, Brenner M, Rosenmeier MF (2007) Quantification of soil erosion rates related to ancient Maya deforestation. *Geology* 35(10):915–918.
27. Hodell DA, Curtis JH, Brenner M (1995) Possible role of climate in the collapse of Classic Maya civilization. *Nature* 375(6530):391–394.
28. Rosenmeier MF, Hodell DA, Brenner M, Curtis JH, Guilderson TP (2002) A 4000-year lacustrine record of environmental change in the southern Maya lowlands, Peten, Guatemala. *Quat Res* 57(2):183–190.
29. Taylor Z, Horn S, Finkelstein D (2013) Maize pollen concentrations in Neotropical lake sediments as an indicator of the scale of prehistoric agriculture. *Holocene* 23(1):78–84.
30. Luna V, et al. (2001) Maize pollen longevity and distance isolation requirements for effective pollen control. *Crop Sci* 41(5):1551–1557.
31. Lane CS, Cummings KE, Clark JJ (2010) Maize pollen deposition in modern lake sediments: A case study from Northeastern Wisconsin. *Rev Palaeobot Palynol* 159(3):177–187.
32. Kennett DJ, et al. (2012) Development and disintegration of Maya political systems in response to climate change. *Science* 338(6108):788–791.

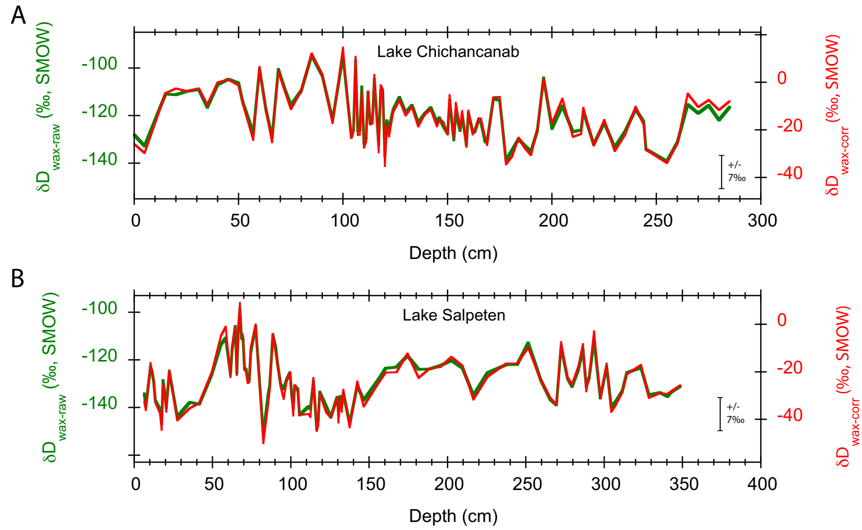

Fig. S1. Comparison of $\delta D_{wax\text{-}raw}$ and $\delta D_{wax\text{-}corr}$ records from Lake Chichancanab (*A*) and Lake Salpeten (*B*). The mean values of the two records are aligned, and the axes are scaled to indicate the same range of variability. Error bars indicate the combined error for $\delta D_{wax\text{-}corr}$ values. The range of variability in the vegetation corrected data ($\delta D_{wax\text{-}corr}$) is not significantly different from the $\delta D_{wax\text{-}raw}$ data for the entirety of both records.

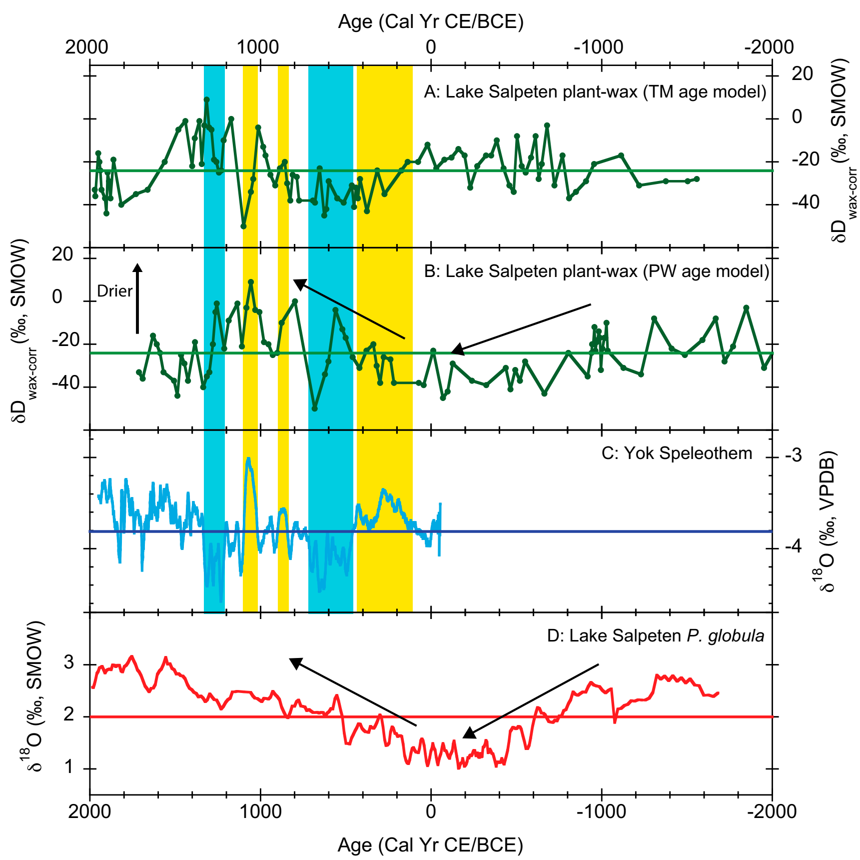

Fig. S2. The Lake Salpeten $\delta D_{wax\text{-}corr}$ record fit to the (*A*) TM age model and (*B*) PW age model compared with hydroclimate proxy records from the southern Maya Lowlands. Horizontal lines indicate the mean value for each record. Colored vertical bars indicate periods of relatively wet (blue) and dry (orange) conditions as recorded by the Yok Speleothem $\delta^{18}O$ record (32) (*C*). Arrows indicate long-term climate trends inferred from the Lake Salpeten ostracod $\delta^{18}O$ record (28) (*D*).

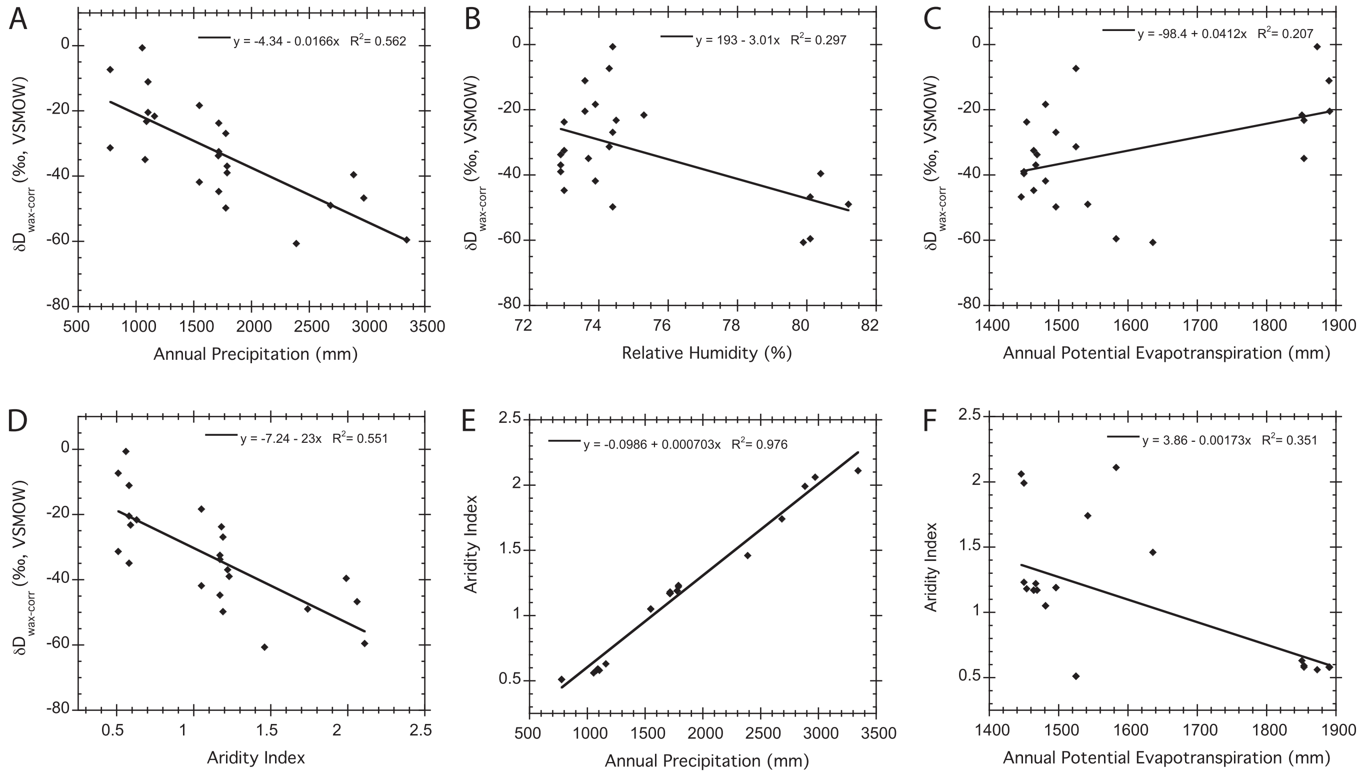

Fig. S3. Scatter plots showing relationships between $\delta D_{wax\text{-}corr}$ and (*A*) annual precipitation (P), (*B*) relative humidity, (*C*) annual PET, and (*D*) the aridity index (AI, defined as P/PET) and relationships between (*E*) AI and P and (*F*) PET. The strongest determinant of $\delta D_{wax\text{-}corr}$ is annual precipitation. A similarly strong relationship is observed between $\delta D_{wax\text{-}corr}$ and AI. Most of the variance in AI at the sampling sites is explained by annual precipitation (*E*), while much less is explained by potential evapotranspiration (*F*), further confirming that precipitation is more important than potential evapotranspiration in controlling spatial variability in $\delta D_{wax\text{-}corr}$.

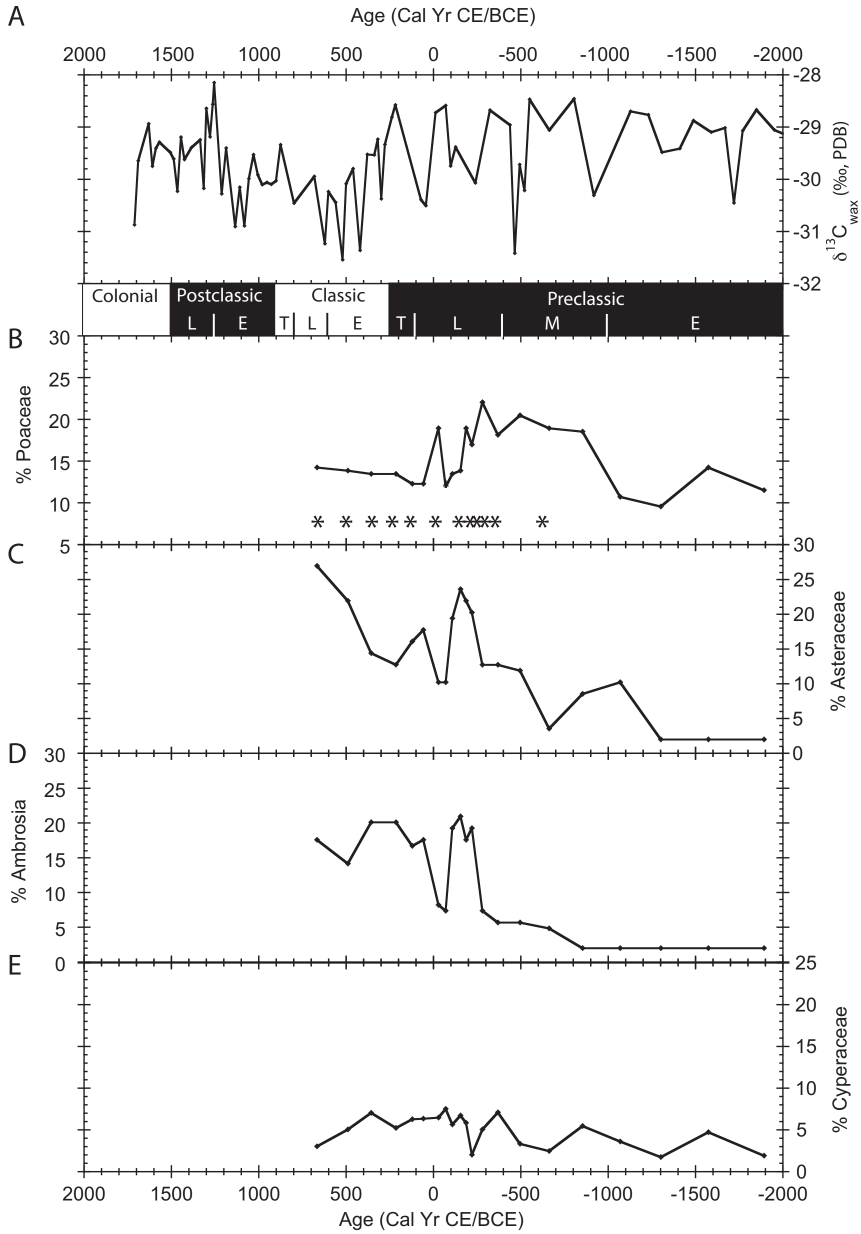

Fig. S4. Comparison of $\delta^{13}C_{wax}$ (*A*) and disturbance pollen records from Lake Salpeten: *Poaceae* (*B*), *Asteraceae* (*C*), *Ambrosia* (*D*), and *Cyperaceae* (*E*) (14). All pollen data are presented as percent of total pollen. Asterisks in *B* indicate the presence of maize (*Zea*) pollen. Pollen data are fit to the age–depth model of ref. 26. The relative abundance of grass (*Poaceae*) pollen decreases beginning in the Late Preclassic, while *Asteraceae* and *Ambrosia* continue to increase through the Classic.

Table S1. Lake Chichancanab plant wax stable isotope data

Depth, cm	TM age 95% CI lower	TM age best, y B.P.	TM age 95% CI upper	PW age 95% CI lower	PW age best, y B.P.	PW age 95% CI upper	$\delta^{13}C$ C26, ‰	$\delta^{13}C$ C28, ‰	$\delta^{13}C$ C30, ‰	$\delta^{13}C$ mean, ‰	f_{c4}	δD C26, ‰	δD C28, ‰	δD C30, ‰	δD mean, ‰	ε_{a}, ‰	δD wax-corr, ‰
0	−75	−58	−49	433	559	654	−27.9	−32.1	−32.8	−30.9	0.39	−147	−104	−134	−128	−105	−26
5	−48	−31	−21	473	588	674	−27.9	−31.3	−31.5	−30.2	0.43	−154	−115	−129	−133	−106	−30
15	3	24	42	547	644	724	−27.4	−30.8	−31.5	−29.9	0.46	−133	−87	−113	−111	−107	−5
20	28	53	75	575	671	751	−26.4	−29.6	−30.1	−28.7	0.53	−127	−90	−116	−111	−109	−3
25	54	83	109	597	698	777	−27.8	−30.7	−31.6	−30.0	0.45	−129	−93	−108	−110	−107	−4
31	86	119	150	619	727	807	−27.5	−30.5	−31.6	−29.9	0.46	−127	−93	−108	−109	−107	−2
35	109	145	178	633	746	827	−27.0	−29.9	−30.7	−29.2	0.50	−128	−101	−121	−116	−108	−9
40	137	177	214	650	768	850	−27.2	−30.8	−31.5	−29.8	0.46	−124	−81	−115	−107	−107	0
45	167	210	250	667	788	871	−28.8	−31.1	−31.6	−30.5	0.42	−120	−87	−107	−105	−106	1
50	199	244	287	683	806	894	−27.6	−31.5	−33.4	−30.8	0.40	−123	−80	−116	−106	−105	−1
52	211	258	301	688	812	903	−27.6	−30.8	−31.9	−30.1	0.44	−133	−84	−125	−114	−106	−9
57	245	294	339	699	827	925	−27.8	−31.4	−32.5	−30.6	0.41	−140	−109	−133	−127	−106	−24
60	265	315	361	706	835	939	−28.1	−31.5	−31.2	−30.3	0.43	−118	−83	−100	−100	−106	6
63	286	337	384	713	842	952	−28.4	−31.5	−29.3	−29.7	0.47	−106	−119	−126	−117	−107	−11
66	307	359	408	721	849	965	−28.2	−30.0	−31.5	−29.9	0.45	−138	−114	−136	−129	−107	−25
69	328	382	431	729	857	977	−28.1	−31.7	−33.2	−31.0	0.39	−116	−74	−112	−101	−105	5
72	351	405	455	738	864	990	−28.6	−31.4	−31.6	−30.6	0.41	−122	−86	−118	−109	−106	−3
75	373	428	479	747	873	1005	−26.6	−29.9	−35.1	−30.5	0.41	−126	−90	−130	−116	−106	−11
80	411	467	519	763	888	1029	−27.9	−30.9	−31.6	−30.1	0.44	−125	−88	−115	−109	−106	−3
85	451	507	560	783	905	1056	−26.0	−30.0	−35.9	−30.6	0.41	−107	−51	−126	−95	−105	12
90	492	548	601	805	927	1084	−28.7	−31.6	−30.9	−30.4	0.42	−112	−74	−123	−103	−106	3
95	534	590	643	833	953	1114	−28.0	−30.4	−31.6	−30.0	0.45	−125	−118	−127	−124	−107	−17
100	577	633	685	865	985	1145	−27.6	−30.2	−30.0	−29.3	0.49	−105	−77	−103	−95	−108	15
102	594	650	702	880	999	1157	−28.7	−31.3	−31.1	−30.4	0.43	−126	−86	−124	−112	−106	−7
104	612	668	720	896	1015	1169	−28.5	−29.7	−29.1	−29.1	0.51	−140	−112	−135	−129	−108	−23
105	621	677	728	904	1023	1176	−28.3	−30.0	−29.8	−29.4	0.49	−140	−104	−133	−126	−108	−20
106	630	686	737	911	1031	1183	−28.4	−31.0	−30.9	−30.1	0.44	−111	−71	−109	−97	−106	11
107	639	694	746	920	1040	1189	−29.2	−30.8	−30.2	−30.1	0.45	−142	−106	−131	−126	−106	−22
108	649	703	755	929	1049	1196	−29.1	−30.9	−30.5	−30.2	0.44	−138	−105	−134	−126	−106	−22
109	658	712	763	938	1058	1203	−29.3	−31.7	−33.0	−31.3	0.37	−122	−82	−119	−108	−104	−4
110	667	721	772	948	1067	1209	−28.8	−30.5	−30.0	−29.8	0.46	−147	−110	−137	−131	−107	−27
111	676	730	781	957	1076	1217	−28.7	−30.8	−29.8	−29.8	0.46	−141	−106	−141	−129	−107	−25
112	686	739	790	966	1086	1224	−28.4	−31.1	−30.3	−29.9	0.45	−123	−92	−116	−110	−107	−4
113	695	748	799	975	1095	1231	−28.3	−30.3	−30.2	−29.6	0.47	−138	−96	−136	−123	−107	−18
114	705	757	808	984	1105	1239	−28.6	−30.2	−30.0	−29.6	0.47	−137	−97	−134	−123	−107	−17
115	714	767	817	994	1115	1246	−27.6	−30.0	−30.8	−29.4	0.49	−116	−77	−121	−105	−108	3
116	723	776	826	1004	1124	1254	−27.9	−29.9	−30.6	−29.5	0.48	−134	−95	−127	−119	−108	−12
117	733	785	834	1013	1134	1261	−29.5	−30.8	−30.8	−30.4	0.43	−142	−119	−135	−132	−106	−29
118	743	794	843	1023	1144	1269	−28.0	−30.4	−28.7	−29.0	0.51	−121	−89	−119	−109	−108	−1
119	752	803	853	1033	1154	1278	−28.4	−29.6	−31.6	−29.9	0.46	−117	−93	−118	−110	−107	−3
120	761	813	862	1044	1164	1287	−29.6	−30.9	−31.3	−30.6	0.41	−149	−126	−135	−137	−106	−35
121	771	822	871	1054	1174	1294	−27.3	−29.9	−34.1	−30.4	0.42	−125	−99	−143	−122	−106	−18
122	781	832	880	1065	1184	1303	−29.0	−31.1	−32.0	−30.7	0.40	−138	−114	−125	−126	−105	−23
124	800	850	898	1086	1203	1322	−28.2	−30.5	−31.5	−30.1	0.45	−128	−103	−122	−118	−106	−12
127	830	879	926	1119	1233	1352	−28.4	−30.9	−32.3	−30.5	0.42	−131	−102	−104	−112	−106	−7
130	860	908	954	1155	1264	1382	−28.1	−30.4	−32.0	−30.2	0.44	−133	−111	−113	−119	−106	−14
133	890	937	982	1191	1296	1414	−27.8	−30.5	−31.8	−30.0	0.45	−129	−100	−118	−116	−107	−10
136	921	967	1010	1230	1329	1448	−28.1	−30.4	−31.8	−30.1	0.44	−137	−114	−118	−123	−106	−19
139	952	996	1038	1271	1364	1484	−27.4	−30.6	−30.7	−29.6	0.48	−133	−106	−119	−119	−107	−13
142	983	1026	1067	1316	1402	1521	−27.9	−30.5	−31.8	−30.1	0.44	−134	−97	−118	−117	−106	−11
145	1014	1057	1096	1363	1443	1558	−28.4	−30.5	−31.2	−30.1	0.45	−140	−112	−118	−123	−106	−18
146	1025	1067	1106	1379	1457	1572	−27.5	−30.1	−31.9	−29.8	0.46	−138	−104	−121	−121	−107	−16
148	1046	1088	1126	1412	1487	1598	−26.5	−28.9	−29.6	−28.3	0.56	−134	−102	−136	−124	−110	−17
150	1067	1108	1146	1447	1518	1626	−26.9	−29.1	−31.8	−29.3	0.50	−138	−111	−134	−127	−108	−22
151	1078	1119	1156	1464	1535	1641	−26.7	−29.3	−30.1	−28.7	0.53	−128	−92	−120	−114	−109	−5
153	1100	1140	1176	1499	1568	1670	−26.3	−29.0	−29.7	−28.3	0.55	−150	−107	−133	−130	−110	−23
154	1110	1150	1186	1516	1585	1686	−26.2	−29.5	−26.9	−27.5	0.60	−131	−101	−125	−119	−111	−9
156	1132	1171	1206	1551	1620	1716	−26.5	−29.2	−30.1	−28.6	0.54	−143	−112	−124	−126	−109	−19
157	1143	1182	1217	1569	1637	1732	−26.5	−30.2	−29.4	−28.7	0.53	−135	−95	−128	−120	−109	−12
159	1165	1203	1238	1605	1674	1763	−27.5	−30.1	−29.6	−29.1	0.51	−153	−106	−138	−132	−108	−27
160	1176	1214	1248	1623	1692	1779	−26.8	−30.5	−29.8	−29.0	0.51	−131	−86	−139	−119	−108	−12

Table S1. Cont.

Depth, cm	TM age 95% CI lower	TM age best, y B.P.	TM age 95% CI upper	PW age 95% CI lower	PW age best, y B.P.	PW age 95% CI upper	$\delta^{13}C$ C26, ‰	$\delta^{13}C$ C28, ‰	$\delta^{13}C$ C30, ‰	$\delta^{13}C$ mean, ‰	f_{c4}	δD C26, ‰	δD C28, ‰	δD C30, ‰	δD mean, ‰	ε_a, ‰	δD wax-corr, ‰
162	1198	1235	1269	1661	1729	1812	−28.2	−30.9	−29.9	−29.6	0.47	−144	−99	−137	−127	−107	−22
163	1209	1246	1280	1678	1748	1829	−25.6	−30.1	−30.4	−28.7	0.53	−141	−104	−136	−127	−109	−20
165	1230	1268	1301	1715	1785	1862	−25.7	−30.0	−31.9	−29.2	0.50	−139	−93	−132	−121	−108	−15
166	1241	1279	1312	1734	1804	1879	−26.1	−29.9	−29.6	−28.5	0.54	−138	−97	−133	−123	−109	−15
168	1264	1300	1334	1770	1842	1913	−25.9	−29.0	−29.1	−28.0	0.58	−146	−112	−135	−131	−110	−23
169	1275	1311	1345	1788	1861	1931	−27.4	−31.1	−30.1	−29.5	0.48	−139	−113	−141	−131	−107	−26
172	1308	1345	1379	1843	1918	1988	−25.9	−29.4	−33.5	−29.6	0.48	−128	−87	−124	−113	−107	−6
175	1341	1378	1413	1896	1974	2048	−26.5	−30.3	−30.5	−29.1	0.50	−129	−89	−122	−114	−108	−6
178	1374	1412	1448	1949	2030	2112	−27.1	−30.1	−30.2	−29.1	0.50	−157	−114	−146	−139	−108	−34
181	1408	1446	1484	2000	2086	2177	−28.9	−30.4	−30.4	−29.9	0.45	−151	−115	−138	−134	−107	−31
184	1441	1481	1521	2052	2143	2243	−27.0	−29.5	−29.2	−28.6	0.54	−146	−106	−137	−130	−109	−23
187	1474	1516	1558	2104	2199	2310	−27.2	−29.2	−31.1	−29.2	0.50	−139	−120	−139	−133	−108	−28
190	1507	1551	1596	2156	2256	2378	−27.5	−29.8	−30.8	−29.4	0.49	−148	−117	−141	−135	−108	−31
193	1541	1586	1635	2210	2314	2444	−26.9	−28.9	−29.9	−28.6	0.54	−135	−110	−134	−126	−109	−19
196	1574	1622	1674	2264	2373	2510	−27.2	−30.0	−34.9	−30.7	0.40	−108	−74	−130	−104	−105	1
200	1619	1670	1727	2338	2453	2597	−25.4	−28.9	−29.9	−28.1	0.57	−146	−105	−122	−124	−110	−17
205	1675	1731	1795	2436	2556	2704	−24.9	−28.6	−31.0	−28.2	0.57	−133	−91	−123	−116	−110	−7
210	1732	1793	1864	2537	2661	2810	−25.7	−31.1	−33.8	−30.2	0.44	−151	−113	−116	−127	−106	−23
214	1777	1843	1920	2619	2747	2893	−27.2	−30.6	−32.1	−30.0	0.45	−145	−109	−124	−126	−107	−22
215	1788	1855	1935	2640	2768	2914	−25.6	−30.4	−30.8	−28.9	0.52	−138	−100	−117	−118	−108	−11
220	1845	1919	2007	2744	2877	3018	−26.3	−30.0	−30.6	−28.9	0.52	−154	−107	−136	−132	−108	−27
225	1902	1983	2080	2848	2988	3122	−26.8	−29.4	−29.9	−28.7	0.53	−145	−106	−118	−123	−109	−16
230	1960	2048	2155	2950	3100	3229	−27.3	−29.9	−31.2	−29.5	0.48	−153	−121	−125	−133	−108	−29
235	2017	2114	2231	3052	3212	3340	−27.9	−30.0	−31.1	−29.7	0.47	−146	−118	−117	−127	−107	−22
240	2075	2181	2308	3155	3325	3451	−27.4	−30.5	−29.4	−29.1	0.50	−135	−94	−123	−117	−108	−10
244	2122	2236	2371	3238	3416	3541	−27.4	−30.6	−32.0	−30.0	0.45	−143	−103	−122	−123	−107	−18
245	2134	2249	2387	3259	3439	3564	−26.0	−29.4	−30.6	−28.7	0.53	−155	−113	−134	−134	−109	−28
255	2257	2390	2558				−26.3	−29.7	−29.9	−28.6	0.54	−159	−118	−141	−139	−109	−34
260							−26.1	−29.8	−30.8	−28.9	0.52	−152	−113	−129	−131	−109	−26
265							−24.6	−28.4	−29.4	−27.5	0.61	−140	−90	−116	−115	−111	−5
270							−25.6	−29.1	−30.0	−28.3	0.56	−140	−100	−117	−119	−110	−10
275							−25.9	−29.5	−30.4	−28.6	0.54	−140	−90	−117	−116	−109	−7
280							−24.5	−28.4	−28.8	−27.2	0.62	−148	−84	−134	−122	−111	−12
285							−25.7	−29.2	−30.3	−28.4	0.55	−138	−92	−119	−116	−109	−8

CI, confidence interval.

Table S2. Lake Salpeten plant wax stable isotope data

Depth, cm	TM age 95% CI lower	TM age best, y B.P.	TM age 95% CI upper	PW age 95% CI lower	PW age best, y B.P.	PW age 95% CI upper	$\delta^{13}C$ C26, ‰	$\delta^{13}C$ C28, ‰	$\delta^{13}C$ C30, ‰	$\delta^{13}C$ mean, ‰	f_{c4}	δD C26, ‰	δD C28, ‰	δD C30, ‰	δD mean, ‰	ε_{a}, ‰	δD wax-corr, ‰
6.5	−50	−22	11	102	238	463	−30.6	−31.2	−30.9	−30.9	0.39	−137	−127	−139	−134	−105	−33
7.5	−46	−18	19	129	259	472	−29.6	−29.6	−29.7	−29.6	0.47	−138	−127	−154	−139	−107	−36
10.5	−34	−1	39	208	320	498	−29.6	−29.0	−28.3	−28.9	0.52	−130	−115	−124	−123	−108	−16
11.5	−29	5	48	234	341	506	−30.4	−29.3	−29.6	−29.8	0.47	−132	−118	−125	−125	−107	−20
12.5	−24	11	55	260	361	514	−29.4	−29.0	−29.8	−29.4	0.49	−136	−122	−130	−129	−108	−24
13.5	−19	18	64	284	381	523	−29.2	−29.5	−29.1	−29.3	0.49	−146	−125	−141	−137	−108	−33
16.5	−2	39	91	359	443	552	−30.2	−29.7	−28.6	−29.5	0.48	−148	−133	−141	−141	−107	−37
17.5	5	47	100	383	463	564	−29.6	−29.5	−29.7	−29.6	0.47	−153	−133	−154	−147	−107	−44
18.5	11	54	110	406	484	578	−30.9	−30.3	−29.5	−30.2	0.43	−137	−120	−129	−129	−106	−25
19.5	18	62	120	429	504	592	−29.8	−29.1	−28.7	−29.2	0.50	−141	−129	−130	−134	−108	−29
20.5	26	71	129	452	524	605	−29.1	−30.0	−29.8	−29.6	0.47	−147	−130	−143	−140	−107	−37
22.5	41	88	150	494	565	638	−30.0	−29.4	−28.8	−29.4	0.49	−136	−115	−124	−125	−108	−19
27.5	83	134	203	544	614	685	−29.3	−29.7	−28.7	−29.2	0.50	−154	−128	−150	−144	−108	−40
35.5	162	219	295	571	635	698	−29.5	−30.7	−30.2	−30.2	0.44	−151	−111	−151	−138	−106	−35
41.5	228	288	367	587	650	713	−28.1	−29.6	−28.2	−28.6	0.54	−152	−112	−152	−139	−109	−33
49.5	326	388	470	609	671	739	−28.7	−29.8	−29.1	−29.2	0.50	−141	−102	−135	−126	−108	−20
55.5	405	468	548	622	686	761	−28.0	−28.9	−28.8	−28.6	0.54	−125	−100	−115	−113	−109	−5
58.5	445	509	587	625	694	775	−28.9	−27.8	−27.7	−28.1	0.57	−127	−96	−109	−111	−110	−1
61.5	488	550	627	670	737	814	−29.4	−30.4	−31.1	−30.3	0.43	−146	−105	−126	−126	−106	−22
62.5	502	564	641	695	763	839	−28.3	−29.5	−30.4	−29.4	0.49	−140	−98	−110	−116	−108	−9
64.5	530	592	669	746	815	889	−30.4	−30.7	−31.7	−30.9	0.39	−133	−92	−92	−106	−105	−1
65.5	544	606	682	770	841	914	−29.5	−30.0	−31.0	−30.2	0.44	−151	−102	−123	−125	−106	−21
66.5	558	620	696	793	867	940	−30.5	−30.8	−31.4	−30.9	0.39	−133	−94	−96	−108	−105	−3
67.5	572	634	710	815	893	967	−29.9	−30.0	−30.0	−30.0	0.45	−128	−85	−82	−99	−107	9
68.5	586	649	724	835	919	995	−29.2	−30.3	−29.0	−29.5	0.48	−138	−94	−101	−111	−107	−4
69.5	600	663	738	855	944	1024	−28.7	−30.2	−30.9	−29.9	0.45	−139	−94	−101	−111	−107	−5
70.5	614	677	752	875	970	1054	−29.4	−30.5	−30.4	−30.1	0.44	−143	−106	−121	−124	−106	−19
71.5	628	691	766	893	996	1085	−29.2	−30.7	−30.3	−30.1	0.45	−147	−107	−119	−124	−106	−20
72.5	642	706	779	912	1022	1116	−29.5	−29.8	−31.0	−30.1	0.44	−151	−111	−123	−128	−106	−25
73.5	656	720	793	931	1048	1148	−29.2	−30.4	−30.4	−30.0	0.45	−149	−111	−125	−128	−107	−24
74.5	670	734	807	949	1074	1180	−28.2	−29.7	−30.1	−29.3	0.49	−138	−94	−117	−116	−108	−10
77.5	712	778	849	1004	1152	1275	−30.0	−29.9	−31.4	−30.5	0.42	−110	−100	−108	−106	−106	0
82.5	784	850	916	1114	1267	1400	−29.0	−29.5	−31.3	−29.9	0.45	−174	−136	−144	−151	−107	−50
85.5	827	893	958	1178	1328	1458	−31.6	−30.0	−32.1	−31.2	0.37	−155	−113	−136	−135	−104	−34
86.5	841	907	973	1200	1348	1478	−29.4	−30.4	−30.9	−30.2	0.43	−154	−114	−126	−131	−106	−28
88.5	869	936	1001	1242	1389	1524	−29.8	−30.5	−31.1	−30.4	0.42	−134	−88	−106	−109	−106	−4
90.5	898	965	1030	1281	1429	1572	−30.3	−31.8	−32.6	−31.5	0.35	−141	−94	−111	−115	−104	−13
91.5	912	979	1043	1300	1449	1597	−28.5	−30.7	−31.0	−30.1	0.44	−147	−101	−116	−121	−106	−17
93.5	941	1008	1072	1334	1490	1652	−29.2	−30.0	−30.2	−29.8	0.46	−158	−114	−119	−130	−107	−26
95.5	970	1036	1102	1369	1530	1704	−31.3	−31.6	−31.2	−31.4	0.36	−152	−114	−130	−132	−104	−31
97.5	998	1064	1131	1396	1571	1758	−29.2	−29.5	−29.8	−29.5	0.48	−139	−108	−137	−128	−107	−23
99.5	1025	1092	1158	1424	1611	1818	−29.4	−30.1	−29.0	−29.5	0.48	−142	−100	−134	−125	−107	−20
100.5	1039	1106	1171	1437	1631	1847	−28.2	−30.7	−28.8	−29.2	0.50	−148	−112	−144	−134	−108	−30
101.5	1184	1124	1120	1452	1651	1876	−30.5	−31.2	−29.5	−30.4	0.43	−158	−118	−145	−140	−106	−38
102.5	1198	1138	1134	1463	1672	1905	−28.9	−30.3	−28.8	−29.3	0.49	−142	−111	−139	−131	−108	−26
104.5	1095	1162	1226	1489	1712	1964	−27.8	−30.0	−28.6	−28.8	0.52	−141	−115	−142	−133	−109	−27
105.5	1109	1176	1240	1502	1732	1995	−28.2	−29.5	−28.0	−28.6	0.54	−155	−126	−149	−143	−109	−38
111.5	1192	1257	1320	1643	1878	2146	−29.9	−31.1	−30.2	−30.4	0.42	−154	−116	−149	−140	−106	−38
112.5	1205	1270	1333	1678	1906	2167	−29.9	−32.0	−29.6	−30.5	0.42	−153	−121	−148	−141	−106	−39
114.5	1232	1297	1361	1747	1962	2208	−27.7	−29.9	−28.5	−28.7	0.53	−144	−110	−133	−129	−109	−23
116.5	1257	1323	1387	1815	2019	2250	−27.7	−29.4	−28.6	−28.6	0.54	−164	−130	−153	−149	−109	−45
117.5	1270	1336	1400	1848	2047	2270	−29.7	−30.1	−29.5	−29.7	0.47	−162	−123	−149	−145	−107	−42
118.5	1283	1349	1412	1883	2076	2291	−29.0	−29.5	−29.7	−29.4	0.49	−155	−109	−137	−134	−108	−29
122.5	1332	1400	1462	2017	2189	2376	−29.5	−30.7	−30.0	−30.1	0.44	−163	−116	−140	−139	−106	−37
125.5	1368	1437	1499	2117	2273	2444	−28.1	−29.2	−28.7	−28.7	0.53	−161	−126	−146	−144	−109	−39
129.5	1417	1485	1556	2251	2387	2535	−28.5	−29.5	−28.9	−29.0	0.52	−155	−117	−135	−136	−108	−31
130.5	1426	1498	1561	2284	2415	2558	−31.4	−31.3	−31.5	−31.4	0.36	−155	−127	−141	−141	−104	−41
131.5	1437	1510	1573	2316	2443	2580	−29.4	−30.6	−29.1	−29.7	0.47	−147	−118	−141	−135	−107	−32
132.5	1448	1521	1586	2350	2471	2604	−30.3	−30.5	−29.8	−30.2	0.44	−138	−130	−150	−139	−106	−37
133.5	1460	1533	1598	2382	2500	2628	−27.3	−29.3	−28.8	−28.5	0.55	−150	−115	−136	−134	−109	−28
137.5	1499	1573	1639	2508	2613	2726	−29.2	−29.4	−28.6	−29.1	0.51	−155	−134	−151	−147	−108	−43

Table S2. Cont.

Depth, cm	TM age 95% CI lower	TM age best, y B.P.	TM age 95% CI upper	PW age 95% CI lower	PW age best, y B.P.	PW age 95% CI upper	$\delta^{13}C$ C26, ‰	$\delta^{13}C$ C28, ‰	$\delta^{13}C$ C30, ‰	$\delta^{13}C$ mean, ‰	f_{c4}	δD C26, ‰	δD C28, ‰	δD C30, ‰	δD mean, ‰	ε_a, ‰	δD wax-corr, ‰
142.5	1558	1634	1702	2658	2754	2868	−27.6	−29.4	−28.3	−28.5	0.55	−150	−111	−131	−131	−109	−24
146.5	1601	1676	1745	2767	2867	2986	−29.8	−31.3	−29.8	−30.3	0.43	−154	−121	−136	−137	−106	−35
156.5	*1699*	*1776*	*1843*	*2794*	*2890*	*3009*	*−29.2*	*−31.0*	*−30.5*	*−30.2*	*0.43*	*−141*	*−110*	*−133*	*−128*	*−106*	*−24*
160.5	*1735*	*1812*	*1879*	*2798*	*2894*	*3012*	*−30.1*	*−31.8*	*−30.2*	*−30.7*	*0.40*	*−133*	*−106*	*−131*	*−124*	*−105*	*−20*
167.5	*1796*	*1873*	*1942*	*2805*	*2900*	*3019*	*−29.8*	*−31.5*	*−31.4*	*−30.9*	*0.39*	*−139*	*−108*	*−122*	*−123*	*−105*	*−20*
174.5	*1850*	*1929*	*2000*	*2810*	*2907*	*3027*	*−28.6*	*−30.6*	*−29.8*	*−29.6*	*0.47*	*−132*	*−102*	*−120*	*−118*	*−107*	*−12*
181.5	*1902*	*1980*	*2054*	*2814*	*2913*	*3032*	*−31.9*	*−30.9*	*−31.9*	*−31.6*	*0.35*	*−134*	*−113*	*−125*	*−124*	*−104*	*−23*
188.5	*1950*	*2027*	*2098*	*2819*	*2920*	*3038*	*−28.3*	*−30.7*	*−30.0*	*−29.7*	*0.47*	*−133*	*−110*	*−128*	*−124*	*−107*	*−19*
195.5	*1995*	*2070*	*2141*	*2823*	*2926*	*3046*	*−29.0*	*−31.3*	*−30.0*	*−30.1*	*0.44*	*−137*	*−107*	*−124*	*−122*	*−106*	*−18*
202.5	*2037*	*2109*	*2180*	*2827*	*2932*	*3056*	*−27.9*	*−30.3*	*−29.4*	*−29.2*	*0.50*	*−133*	*−107*	*−121*	*−120*	*−108*	*−14*
209.5	*2076*	*2146*	*2216*	*2831*	*2939*	*3066*	*−28.2*	*−30.5*	*−29.3*	*−29.3*	*0.49*	*−134*	*−113*	*−124*	*−123*	*−108*	*−17*
216.5	*2113*	*2179*	*2249*	*2834*	*2945*	*3076*	*−28.7*	*−31.0*	*−30.2*	*−30.0*	*0.45*	*−149*	*−122*	*−134*	*−135*	*−107*	*−32*
225.5	*2158*	*2220*	*2289*	*2838*	*2954*	*3091*	*−29.4*	*−31.7*	*−30.5*	*−30.5*	*0.42*	*−139*	*−114*	*−123*	*−125*	*−106*	*−22*
237.5	*2209*	*2272*	*2341*	*2844*	*2965*	*3112*	*−28.3*	*−31.0*	*−29.5*	*−29.6*	*0.48*	*−141*	*−100*	*−125*	*−122*	*−107*	*−17*
244.5	*2238*	*2302*	*2375*	*2846*	*2971*	*3125*	*−28.6*	*−30.3*	*−30.2*	*−29.7*	*0.47*	*−143*	*−94*	*−129*	*−122*	*−107*	*−17*
251.5	*2268*	*2335*	*2408*	*2849*	*2978*	*3140*	*−30.5*	*−31.4*	*−32.4*	*−31.4*	*0.36*	*−128*	*−99*	*−111*	*−113*	*−104*	*−10*
259.5	*2305*	*2375*	*2451*	*2852*	*2985*	*3156*	*−28.4*	*−30.7*	*−29.4*	*−29.5*	*0.48*	*−145*	*−109*	*−131*	*−128*	*−107*	*−23*
265.5	2339	2409	2483	2948	3077	3245	−28.0	−29.9	−28.3	−28.7	0.53	−150	−121	−139	−137	−109	−31
269.5	2362	2434	2508	3056	3180	3340	−28.3	−29.5	−28.4	−28.8	0.53	−153	−120	−144	−139	−109	−34
272.5	2380	2453	2529	3137	3257	3412	−28.6	−31.0	−28.9	−29.5	0.48	−133	−92	−118	−114	−108	−8
276.5	2406	2481	2557	3245	3360	3507	−28.8	−30.0	−29.4	−29.4	0.49	−146	−106	−131	−128	−108	−22
279.5	2428	2504	2580	3325	3437	3579	−27.9	−29.9	−28.8	−28.9	0.52	−148	−106	−139	−131	−109	−25
283.5	2460	2536	2610	3432	3540	3675	−28.7	−29.9	−28.7	−29.1	0.51	−144	−100	−129	−124	−108	−18
286.5	2487	2562	2637	3513	3618	3750	−27.9	−30.3	−28.9	−29.0	0.51	−132	−91	−124	−116	−108	−8
288.5	2505	2580	2654	3567	3669	3800	−29.7	−31.3	−30.4	−30.5	0.42	−146	−111	−136	−131	−106	−28
290.5	2524	2599	2674	3621	3720	3852	−29.0	−29.4	−28.9	−29.1	0.51	−131	−113	−138	−127	−108	−21
293.5	2554	2630	2703	3700	3798	3929	−27.9	−29.1	−29.0	−28.7	0.53	−129	−87	−119	−112	−109	−3
297.5	2599	2673	2744	3805	3901	4037	−28.5	−30.1	−28.5	−29.1	0.51	−149	−120	−140	−136	−108	−31
301.5	2647	2720	2789	3911	4003	4148	−28.0	−30.4	−29.1	−29.2	0.50	−142	−103	−124	−123	−108	−17
304.5	2686	2759	2825	3989	4081	4232	−29.9	−30.2	−29.7	−29.9	0.46	−148	−122	−149	−140	−107	−37
307.5	2726	2799	2866	4067	4158	4318	−28.6	−31.0	−29.3	−29.6	0.47	−148	−118	−146	−137	−107	−34
311.5	2787	2858	2923	4170	4261	4432	−28.9	−29.9	−29.3	−29.4	0.49	−150	−111	−139	−133	−108	−29
314.5	2836	2905	2968	4248	4338	4517	−29.1	−31.0	−29.6	−29.9	0.45	−146	−105	−126	−125	−107	−21
323.5	3000	3064	3133	4480	4569	4775	−28.2	−30.3	−29.3	−29.2	0.50	−142	−101	−127	−123	−108	−17
328.5	3109	3169	3246	4606	4698	4919	−28.9	−30.1	−30.3	−29.8	0.46	−157	−112	−135	−135	−107	−31
335.5	3265	3325	3424	4781	4878	5115	−28.6	−29.6	−29.6	−29.3	0.49	−167	−102	−132	−134	−108	−29
340.5	3384	3453	3571				−28.1	−28.9	−28.4	−28.5	0.55	−163	−107	−136	−135	−109	−29
342.5	3433	3507	3629				−29.0	−29.3	−28.8	−29.0	0.51	−154	−109	−137	−134	−108	−28
348.5							−28.6	−29.4	−29.2	−29.1	0.51	−163	−101	−129	−131	−108	−26

Italics indicate core interval with minimal change in the PW age model. These data are not interpreted in terms of past environmental change. CI, confidence interval.

Table S3. Compound-specific radiocarbon results from Lake Salpeten

NOSAMS sample number	Sediment core depth, cm	$\Delta^{14}C_{wax}$, ‰	Error, ‰	2σ lower Cal age, y B.P.	Median Cal age, y B.P.	2σ upper Cal age, y B.P.	$\delta^{13}C_{CO2}$, ‰	$\delta^{13}C_{GC\text{-}IRMS}$, ‰
88449	0.5–5.5	−8	18	−5	161	426	−32.9	
88551	23.5–25.5	−76	10	523	609	697	−32.8	
88453	59.5–60.5	−94	7	564	712	782	−29.5	
107434	75–85	−155	10	1,058	1,296	1,362	−32.2	−31.9
88455	106.5–110.5	−212	14	1,535	1,866	2,104	−28.4	
107435	143–150	−299	7	2,780	2,916	3,057	−32.0	−31.7
107436	258–265	−300	9	2,777	2,990	3,141	−31.9	−31.9
88463	338.5–339.5	−425	5	4,853	4,935	5,256	−29.7	

Cal, calendar.